Research Article | Vol. 26, No. 9 | 30 Apr 2018 | OPTICS EXPRESS 11718
Optics EXPRESS

Direct fabricating large-area nanotriangle structure arrays on tungsten surface by nonlinear lithography of two femtosecond laser beams

QI LIU,[1] NAN ZHANG,[1,5] JIANJUN YANG,[1,2,6] HONGZHEN QIAO,[3] AND CHUNLEI GUO[2,4]

[1]*Institute of Modern Optics, Nankai University, Tianjin 300350, China*
[2]*State Key Laboratory of Applied Optics,Changchun Institute of Optics, Fine Mechanics and Physics, Chinese Academy of Sciences, Changchun 130033, China*
[3]*School of Electronic and Electrical Engineering, Shangqiu Normal University, Henan 476000, China*
[4]*The Institute of Optics, University of Rochester, Rochester, NY 14627, USA*
[5]*zhangn@nankai.edu.cn*
[6]*jjyang@nankai.edu.cn*

Abstract: Two-dimensional arrays of periodic nanostructures are fabricated on bulk tungsten surface within a single step using collinear propagation of two time-delayed femtosecond laser beams with orthogonal polarizations. It is surprisingly found that the geometric profile of the structure unit exhibits a triangle shape in hundred nanometer scales, and its spatial dimension can be modulated by the ambient air pressure ranging from 1 atm to 10^{-3} Pa. As the ambient air pressure decreases, the obtained surface structures display a large depth covered with nanowires. Physically, the formation of such triangle structures is originated from the transient physical correlations between the two laser-matter interaction processes, and also affected by the heat transfer effects of the surrounding air. In addition, the experimental measurements reveal that the minimum reflectivity of the nanotriangle surface structures is unprecedentedly reduced to as low as ~2.9% especially within the visible-infrared range.

OCIS codes: (140.3390) Laser materials processing; (320.7120) Ultrafast phenomena; (310.6628) Subwavelength structures, nanostructures; (160.3900) Metals.

References and links

1. A. Y. Vorobyev and C. Guo, "Multifunctional surfaces produced by femtosecond laser pulses," J. Appl. Phys. **117**(3), 033103 (2015).
2. Y. Yang, J. Yang, C. Liang, and H. Wang, "Ultra-broadband enhanced absorption of metal surfaces structured by femtosecond laser pulses," Opt. Express **16**(15), 11259–11265 (2008).
3. A. Y. Vorobyev, V. S. Makin, and C. Guo, "Brighter light sources from black metal: significant increase in emission efficiency of incandescent light sources," Phys. Rev. Lett. **102**(23), 234301 (2009).
4. Y.-H. Tan, K. Yu, J.-Z. Li, H. Fu, and Z.-Q. Zhu, "MoS_2@ZnO nano-heterojunctions with enhanced photocatalysis and field emission properties," J. Appl. Phys. **116**(6), 064305 (2014).
5. J. Yong, F. Chen, Q. Yang, and X. Hou, "Femtosecond laser controlled wettability of solid surfaces," Soft Matter **11**(46), 8897–8906 (2015).
6. M. Kulkarni, A. Mazare, E. Gongadze, Š. Perutkova, V. Kralj-Iglič, I. Milošev, P. Schmuki, A Iglič, and M. Mozetič, "Titanium nanostructures for biomedical applications," Nanotechnology **26**(6), 062002 (2015).
7. S. Kim, B. Marelli, M. A. Brenckle, A. N. Mitropoulos, E. S. Gil, K. Tsioris, H. Tao, D. L. Kaplan, and F. G. Omenetto, "All-water-based electron-beam lithography using silk as a resist," Nat. Nanotechnol. **9**(4), 306–310 (2014).
8. V. Rinnerbauer, S. Ndao, Y. X. Yeng, J. J. Senkevich, K. F. Jensen, J. D. Joannopoulos, M. Soljačić, I. Celanovic, and R. D. Geil, "Large-area fabrication of high aspect ratio tantalum photonic crystals for high-temperature selective emitters," J. Vac. Sci. Technol. B **31**(1), 011802 (2013).
9. L. A. Ibbotson, A. Demetriadou, S. Croxall, O. Hess, and J. J. Baumberg, "Optical nano-woodpiles: large-area metallic photonic crystals and metamaterials," Sci. Rep. **5**(1), 8313 (2015).
10. E. Stankevičius, M. Garliauskas, M. Gedvilas, N. Tarasenko, and G. Račiukaitis, "Structuring of surfaces with gold nanoparticles by using bessel-like beams," Ann. Phys. **529**(12), 1700174 (2017).

#325332 https://doi.org/10.1364/OE.26.011718
Journal © 2018 Received 2 Mar 2018; revised 17 Apr 2018; accepted 18 Apr 2018; published 23 Apr 2018

Optics EXPRESS

11. E. Stankevičius, M. Garliauskas, and G. Račiukaitis, "Bessel-like beam array generation using round-tip microstructures and their use in the material treatment," J. Laser Micro Nanoeng. **11**(3), 352–356 (2016).
12. M. Gedvilas, J. Mikšys, and G. Račiukaitis, "Flexible periodical micro-and nano-structuring of a stainless steel surface using dual-wavelength double-pulse picosecond laser irradiation," RSC Advances **5**(92), 75075–75080 (2015).
13. F. Chen and J. R. V. de Aldana, "Optical waveguides in crystalline dielectric materials produced by femtosecond-laser micromachining," Laser Photonics Rev. **8**(2), 251–275 (2014).
14. Y. Yang, J. Yang, L. Xue, and Y. Guo, "Surface patterning on periodicity of femtosecond laser- induced ripples," Appl. Phys. Lett. **97**(14), 141101 (2010).
15. G. Miyaji and K. Miyazaki, "Nanoscale ablation on patterned diamond-like carbon film with femtosecond laser pulses," Appl. Phys. Lett. **91**(12), 123102 (2007).
16. R. Kuladeep, C. Sahoo, and D. N. Rao, "Direct writing of continuous and discontinuous sub-wavelength periodic surface structures on single-crystalline silicon using femtosecond laser," Appl. Phys. Lett. **104**(22), 222103 (2014).
17. J. Bonse, J. Krüger, S. Höhm, and A. Rosenfeld, "Femtosecond laser-induced periodic surface structures," J. Laser Appl. **24**(4), 042006 (2012).
18. S. Sakabe, M. Hashida, S. Tokita, S. Namba, and K. Okamuro, "Mechanism for self-formation of periodic grating structures on a metal surface by a femtosecond laser pulse," Phys. Rev. B **79**(3), 033409 (2009).
19. A. Pan, J. Si, T. Chen, C. Li, and X. Hou, "Fabrication of two-dimensional periodic structures on silicon after scanning irradiation with femtosecond laser multi-beams," Appl. Surf. Sci. **368**, 443–448 (2016).
20. H. Qiao, J. Yang, F. Wang, Y. Yang, and J. Sun, "Femtosecond laser direct writing of large-area two-dimensional metallic photonic crystal structures on tungsten surfaces," Opt. Express **23**(20), 26617–26627 (2015).
21. J. Cong, J. Yang, B. Zhao, and X. Xu, "Fabricating subwavelength dot-matrix surface structures of molybdenum by transient correlated actions of two-color femtosecond laser beams," Opt. Express **23**(4), 5357–5367 (2015).
22. L. Wang, Q.-D. Chen, X.-W. Cao, R. Buividas, X. Wang, S. Juodkazis, and H.-B. Sun, "Plasmonic nano-printing: large-area nanoscale energy deposition for efficient surface texturing," Light Sci. Appl. **6**(12), e17112 (2017).
23. V. M. Andreev, A. S. Vlasov, V. P. Khvostikov, O. A. Khvostikova, P. Y. Gazaryan, S. V. Sorokina, and N. A. Sadchikov, "Solar thermophotovoltaic converters based on tungsten emitters," J. Sol. Energy Eng. **129**(3), 298–303 (2007).
24. Q. Sun, F. Liang, R. Vallée, and S. L. Chin, "Nanograting formation on the surface of silica glass by scanning focused femtosecond laser pulses," Opt. Lett. **33**(22), 2713–2715 (2008).
25. P. Fan, B. Bai, J. Long, D. Jiang, G. Jin, H. Zhang, and M. Zhong, "Broadband high-performance infrared antireflection nanowires facilely grown on ultrafast laser structured Cu surface," Nano Lett. **15**(9), 5988–5994 (2015).
26. Y. Shen, J. Tao, H. Tao, S. Chen, L. Pan, and T. Wang, "Nanostructures in superhydrophobic Ti6Al4V hierarchical surfaces control wetting state transitions," Soft Matter **11**(19), 3806–3811 (2015).
27. S. Bashir, M. S. Rafique, and W. Husinsky, "Femtosecond laser-induced subwavelength ripples on Al, Si, CaF_2 and CR-39," Nucl. Instrum. Meth. B **275**, 1–6 (2012).
28. Z. Chen, "Grating Coupled Surface Plasmons in Metallic Structures," [D]. the University of Exeter as a thesis for the degree of Doctor of Philosophy in Physics, (2007).
29. D. E. Grady, "The spall strength of condensed matter," J. Mech. Phys. Solids **36**(3), 353–384 (1988).
30. J. Xu, X. Xiao, F. Ren, W. Wu, Z. Dai, G. Cai, S. Zhang, J. Zhou, F. Mei, and C. Jiang, "Enhanced photocatalysis by coupling of anatase TiO_2 film to triangular Ag nanoparticle island," Nanoscale Res. Lett. **7**(1), 239 (2012).
31. W.-H. Yang, G. C. Schatz, and R. P. Van Duyne, "Discrete dipole approximation for calculating extinction and Raman intensities for small particles with arbitrary shapes," J. Chem. Phys. **103**(3), 869–875 (1995).
32. Y. Yang, S. Matsubara, L. Xiong, T. Hayakawa, and M. Nogami, "Solvothermal synthesis of multiple shapes of silver nanoparticles and their SERS properties," J. Phys. Chem. C **111**(26), 9095–9104 (2007).

1. Introduction

In recent years specific distribution of micro and nano-structures on the material surfaces has attracted great attention because it can modify the physical-chemistry properties of the target, which provides bright prospects for fundamental research and a wide range of possible applications, such as enhanced optical absorption [1,2], improved thermal or field emission [3,4], and increased hydrophobicity and biocompatibility [5,6]. The fabrication of such structures mostly depends on several techniques, such as electron beam lithography [7], reactive ion beam etching [8], nano-imprinting [9], laser interference lithography [10,11] and laser-induced periodic surface structures (LIPSSs), including those induced by dual-wavelength double-pulse laser irradiation [12]. However, all of these techniques are time-consuming and need costly, sophisticated equipment or templates, which is evidently

Optics EXPRESS

unsuitable for large-area fabrication processes. On the other hand, the femtosecond laser has been identified as possessing the capability to induce the periodic subwavelength surface structures within a beam spot via the self-assembly process, which has been successfully performed on a variety of materials including metals, semiconductors, and dielectrics [13–16], and may present potential routes for one-step nanofabrication of large areas. Nevertheless, most previous studies were concentrated on the generation of one-dimensional (1D) periodic structures on material surfaces in both theory and experiment [17,18]. In contrast, two-dimensional (2D) arrays of periodic nanostructures can provide more versatile functions [19–21], thus its direct generation, especially on the highly absorptive solids, is very important and becomes a challenge for femtosecond laser microprocessing.

In this paper, we use two collinearly propagated femtosecond laser beams with orthogonal polarization and a time delay of 1.2 ps to irradiate the hard material surface of tungsten under different ambient air pressure conditions. First, 2D periodic arrays of nanoscale triangular structures are directly formed on the target surface, and the geometric dimensions of the unit cell can be altered by adjusting the ambient air pressure. Then the optical absorption properties of the fabricated surface structures are characterized by the spectral reflectivity. Finally, the underlying mechanisms of the experimental phenomena are analyzed comprehensively.

2. Experimental setup

The experimental setup is schematically shown in Fig. 1. The horizontally polarized 50 fs Gaussian laser pulses with a central wavelength of 800 nm were generated by a Ti:sapphire femtosecond laser amplifier system (Spitfire, Spectra-physics Inc.) at a repetition rate of 1 kHz. The laser pulse energy can be attenuated by neutral density filters. The temporal splitting of each laser pulse was carried out by transmitting through a 1.26-mm-thick birefringent optical crystal YVO_4, which results in collinearly propagated two femtosecond laser pulses of orthogonal polarization with a time delay of 1.2 ps defined by the crystal thickness. The optical axis of the birefringent crystal was adjusted to an angle of $\theta = 45°$ with respect to the direction of the incident laser polarization, leading to an identical pulse energy of 0.06 mJ and the corresponding laser fluence of 22.9 mJ/cm^2 for two laser sub-pulses.

After passing through an optical window of a vacuum chamber, the two time-delayed laser pulses were focused by a fused silica plano-convex cylindrical lens with a focal length of 50 mm, and stroke onto a tungsten plate (Goodfellow Inc.) at normal incidence. The employment of a cylindrical lens can dramatically increase the throughput of surface modifications [22]. The sample material has dimensions of 25 mm × 25 mm × 1 mm and its surface is placed 0.2 mm before the focus, resulting in an elliptical-shaped beam spot (the length of semi-major axis is ~4.5 mm). Before the experiments, the sample surface was mechanically polished with different grades of sandpapers and ultrasonically washed with acetone. The selection of bulk tungsten as the sample is based on its unique high temperature endurance (>1000K) for potential applications in the emerging field of energy conversion. For example, tungsten material can be used as the absorber or emitter in solar thermophotovoltaic and radioisotope thermophotovoltaic generators [23].

Optics EXPRESS

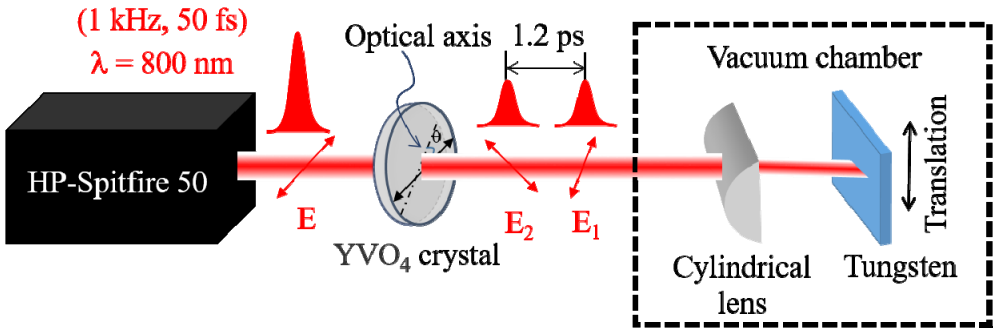

Fig. 1. Schematic diagram of the experiment for the direct fabrication of 2D nanotriangle structure arrays on tungsten surface under a vacuum environment, where two collinear time-delayed (1.2 ps) femtosecond laser beams with orthogonal polarizations are generated from a birefringent optical crystal YVO_4, and a cylindrical lens is employed for the laser focusing. The double-headed arrows represent the direction of the linear polarization of femtosecond laser pulses. $\theta = 45°$ denotes the angle between the optical axis of the birefringent crystal and the polarization direction of the incident laser.

The sample was mounted on a computer-controlled three-dimensional translation stage (WNSC 400, Winner Optical Ltd.) with a resolution of 1 μm. During the experiments, the sample was moved with a speed of 0.06 mm/s along the direction perpendicular to the major axis of the elliptical focal beam spot. The experiments of femtosecond laser fabrication were carried out in the vacuum chamber with different air pressures ranging from 1 atm to 10^{-3} Pa. The morphology of the laser-exposed surface was examined by scanning electron microscopy (SEM) (VE 9800, KEYENCE Inc.) and atomic force microscopy (AFM) (Dimension 3100, BRUKER Inc.).

3. Results and discussions

Figure 2 shows SEM images of the surface morphology after irradiation by two time-delayed femtosecond laser beams of orthogonal polarization under different ambient air pressures of 1 atm, 10^3 Pa and 10^{-3} Pa, respectively. From Fig. 2(a) and its corresponding zoomed-in picture, we can find that the regular 2D arrays of structures can be generated on the tungsten surface under 1 atm, and the geometric profile of the structure unit cells presents a triangle, with three almost equal side-lengths of 405 nm. On the other hand, the formation of each triangle structure unit can be recognized from the cross-cutting behaviors of three nanogrooves oriented along different directions (marked by the green lines in the zoomed-in picture). The measured width of each groove is only 106 nm. From this perspective, we can understand that the distribution of the nanotriangle structure arrays is indeed made by the spatial intersections of three different groups of parallel nanogrooves. The groove periodicity of each group approximates 710 nm, less than the incident laser wavelength. More interestingly, if we have a viewpoint at an intersection point of three nonparallel nanogrooves, a surface pattern of hexagon seems to be constituted by the six surrounding triangle structures. To the best our knowledge, it is for the first time to achieve such unique structures by the maskless fabrication of two collinear propagation of femtosecond laser beams.

Optics EXPRESS

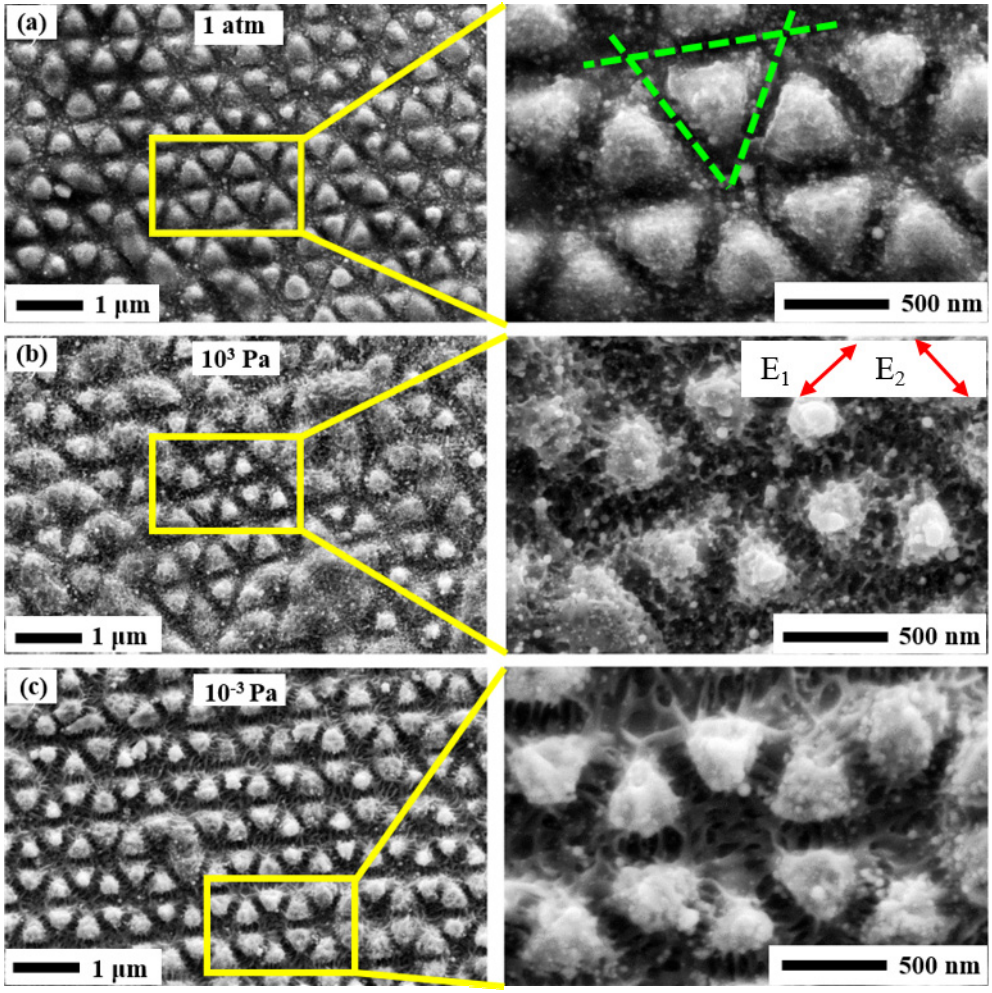

Fig. 2. SEM images of the 2D nanotriangle structure arrays on tungsten surface directly fabricated by two collinear time-delayed femtosecond laser beams of orthogonal polarization. (a), (b) and (c) represent situations under different air pressures of 1 atm, 10^3 Pa and 10^{-3} Pa, respectively.

When the ambient air pressure was reduced to 10^3 Pa, the morphology of the laser-exposed surface also exhibits 2D arrays of nanotriangle structures, as shown in Fig. 2(b), where the distribution of nanoparticles become more intense and short nanowires begin to appear on the bottom of the nanogrooves. In this case, although there are still three groups of parallel lines ablated on the surface, each triangle structure unit become less sharp in the vertexes and have large roughness on the sides. Meanwhile, the side lengths of the triangle decrease to ~355 nm. When the air pressure continues to decrease to as small as 10^{-3} Pa, the 2D triangle arrays are seen evidently with nanowires formation on the bottom of the grooves, which is shown in Fig. 2(c). Similar to the observations under the condition of 10^3 Pa, each triangle structure unit appears to have less sharp edges. However, the highly magnified picture shows the evident formation of nanowires in the groove regions, whose combination with the triangle-shaped structures constitutes an appearance of hierarchical textures. It was also found that the groove period tended to increase when the faster scanning speeds were employed under the same air pressure, being similar to the previous report in silica glass [24]. Noticeably, different from the previous studies with a two-step fabrication method [25,26], it

Optics EXPRESS

is clear that our one-step processing method displays some advantages in convenient and efficient fabrication of hierarchical surface nanostructures. Figure 3 shows the formation of 2D arrays of nanotriangle structures on the extended surface areas when the sample was scanned within the ambient air pressure of 10^{-3} Pa. In the experiments, a surface area of 0.05 mm^2 containing ~1.5×10^5 nanotriangle structures can be fabricated with time about 1 s, which reveals the capability of large-area fabrication for our approach.

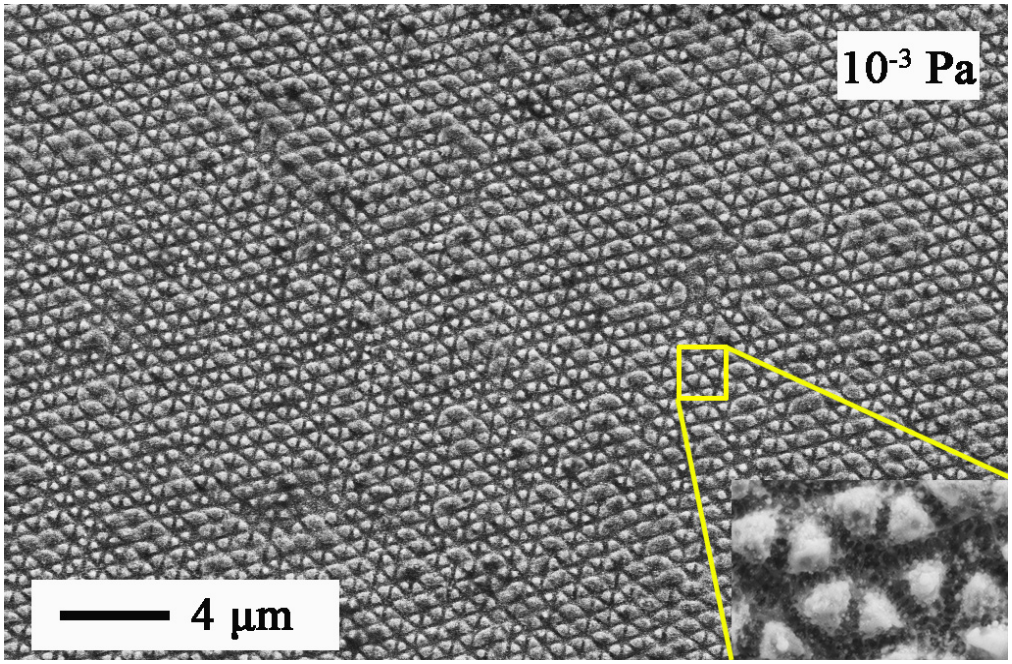

Fig. 3. SEM image of large-area 2D nanotriangle structure arrays on tungsten surface fabricated by femtosecond laser pulses under air pressure of 10^{-3} Pa.

In addition, we also analyzed the cross-section profiles of such 2D surface structure arrays via AFM, and the examined region is indicated by a red line in Fig. 4(a). The measurement results are shown in Fig. 4(b). It can be seen that for each measured profile of the ablation depth there are two types of dips with small and large values (indicated by *d* and *D*) respectively, which corresponds to an individual nanogroove and an intersection point of three nanogrooves. With the decrease of the ambient air pressure, the two values of *d* and *D* both gradually increase. The measured dependences of the ablation depths for both the individual groove and the intersection point of three grooves on the ambient air pressure are plotted in Figs. 4(c) and 4(d), respectively.

Optics EXPRESS

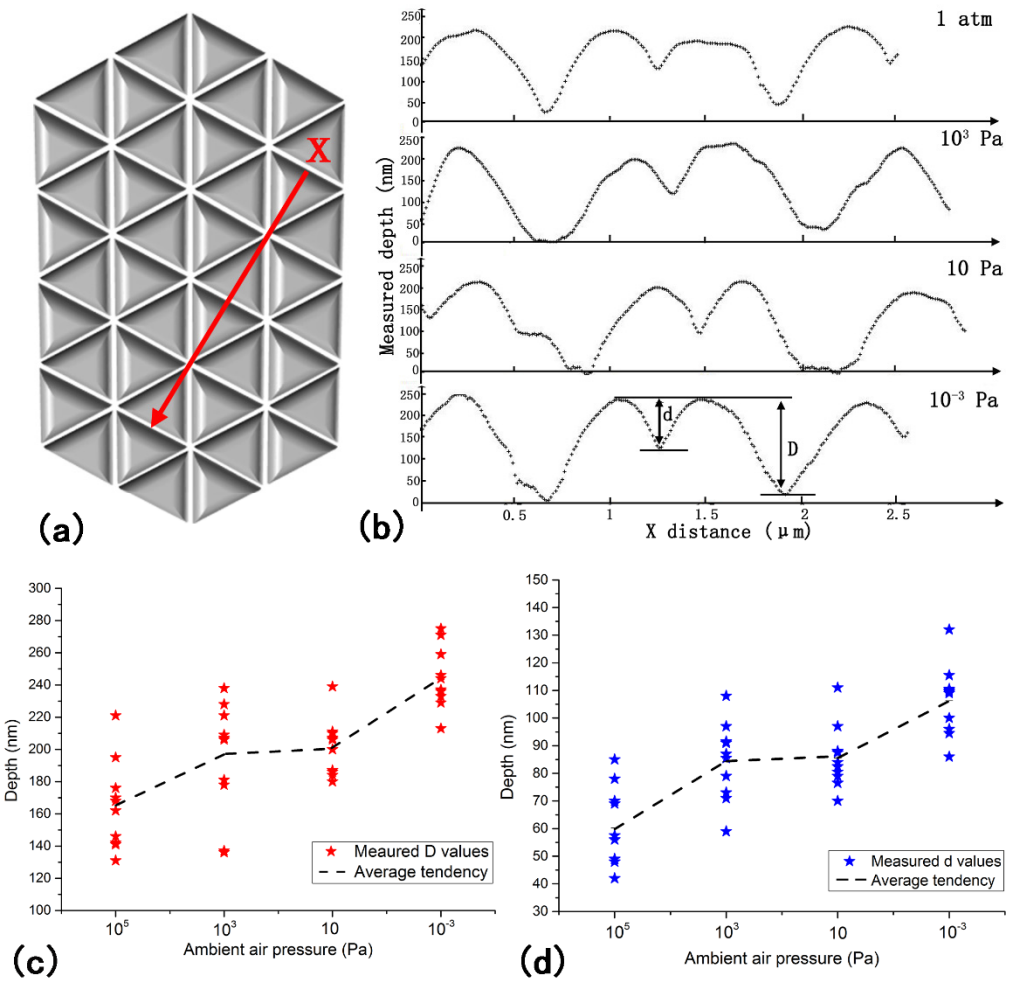

Fig. 4. (a) Schematic of the examined region (red line along X direction) on the sample surface covered with arrays of triangle structures; (b) Measured cross-sectional profiles for the surface structures obtained under several different air pressures, where *d* and *D* denote the depth of the individual groove and the intersection point of three grooves, respectively; (c) Measured dependence of the depth *D* on the ambient air pressure; (d) Measured dependence of the depth *d* on the ambient air pressure.

For each ambient air pressure, measurements (represented by stars) were obtained at several different positions on the structure area, and their average values (represented by dotted lines) can show the change tendencies. Clearly, both the variations of two depths tend to increase with lower ambient air pressure. For example, under 1 atm, 10^3 Pa, 10 Pa and 10^{-3} Pa conditions, the measured average value of *D* is ~165 nm, ~197 nm, ~201 nm and ~244 nm, respectively; while the average value of *d* is ~60 nm, ~84 nm, ~86 nm and ~106 nm, respectively. For the case of each air pressure, the groove periods were measured at 20 different locations on the structured target surface, and the average value shows no definite variation tendency with decreasing the ambient air pressure.

Optics EXPRESS

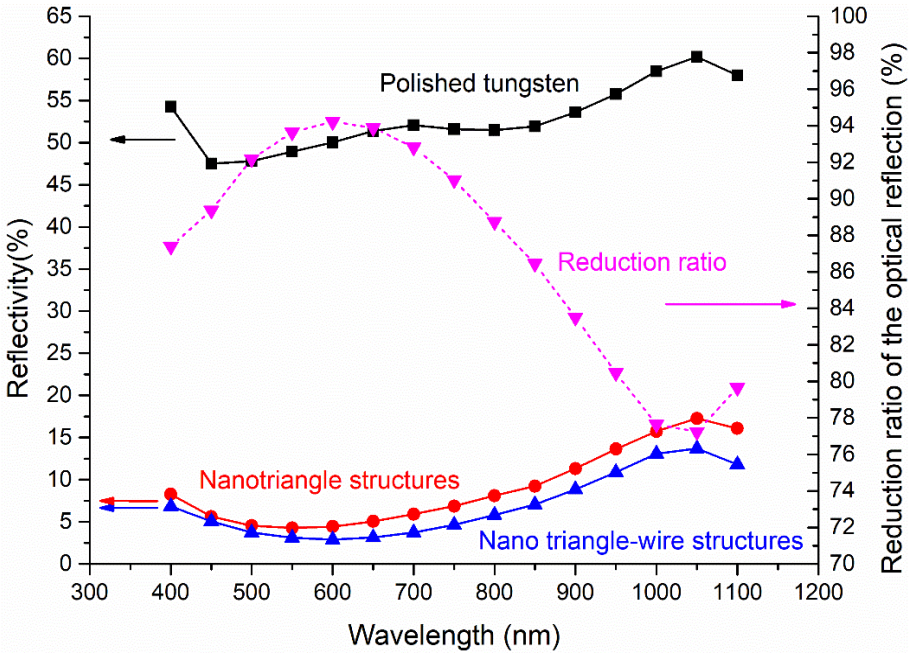

Fig. 5. Measured reflection spectra of tungsten surfaces with different conditions, where the black line represents the polished surface without the laser treatments, the red and blue lines for the triangle surface structures obtained under the pressure of 1 atm and 10^{-3} Pa, respectively. The pink curve shows the reflectivity reduction ratio of the structured surface produced under 10^{-3} Pa to the polished surface.

In order to characterize the optical properties of the tungsten surface with 2D arrays of nanotriangle structures produced by femtosecond laser pulses, we employed a highly sensitive spectrometer (NOVA, ideaoptics Inc.) to measure the spectral reflectivity in the wavelength range of 400 nm-1100 nm, in which the light reflected from the surface is collected by an objective (20 × , NA = 0.4). First, the optical reflectivity of the polished sample surface was measured for comparison, which agrees well with the report in the previous literature [3]. Then we measured the optical reflectivities of the structured sample under two air pressure conditions of 1 atm and 10^{-3} Pa, which were found to have apparently drastic decreases. Remarkably, during the visible wavelength range the measured minimum reflectivity can reach only 4.3% for the surface covered with nanotriangle structure arrays, and even as small as 2.9% for the surface covered with hierarchical structures of nanotriangles and nanowires. This is probably the lowest reflectivity value for the measurement of a tungsten surface. Because the surface microstructuring was performed with air environment of different pressures, some tungsten oxides may be formed on the laser-exposed surface. The Raman measurements revealed that the tungsten oxide compound WO_3 is present on the laser irradiated surface, which becomes less with the decreased air pressure. However, Fig. 5 shows that the reflectance of the structured surface is also decreased with lower air pressures, which indicates that the measured low reflectance cannot be attributed to the oxide compound WO_3 on the tungsten surface. In Fig. 5, the dashed line indicates the calculated ratio of reflectivity reduction for the tungsten surface structured under the air pressure of 10^{-3} Pa with respect to the polished one, which has a maximum value of about 94% at the wavelength of 600 nm. The discrepancy between the measured reflection spectra of the two structured surfaces seems to gradually increase with longer wavelengths.

The experimental observations are discussed as follows: first, we try to elucidate the formation mechanisms of such 2D nanotriangle arrays, which can be boiled down to an

Optics EXPRESS

understanding of the growth of three groups of periodic nanogrooves. When collinear propagation of two time-delayed femtosecond laser beams irradiate the target, the first laser beam can induce a spatially periodic distribution of laser intensity due to interference between the incident light and its excited surface plasmons [27], whose energy deposition subsequently leads to the spatially periodic modification of the properties on the material surface, i.e. a meta-grating surface with the transiently periodic refractive index distribution is achieved, whose grating wave vector $\vec{k}_g$ is parallel to the direction of the first laser pulse polarization. This effect provides a prototype for the latter formation of one group of periodic nanogroove patterns. In addition, because the interpulse time delay is set only 1.2 ps, the incident second femtosecond laser beam linearly polarized in another direction is expected to couple with the above mentioned transient meta-grating surface before its relaxing disappearance. That is, the surface plasmon excitation of the second laser pulse takes place due to the surface roughness, associated with a wave vector $\vec{k}_{spp}$ parallel to the polarization direction of the second laser pulses, which is perpendicular to the transient meta-grating's vector $\vec{k}_g$. By considering the modifications of the transient meta-grating (periodic index change) on the wave front of the propagating surface plasmon induced by the second laser pulse, $\vec{k}_{spp}$ is ready to diffract into two surface plasmons with different wave vectors $\vec{k}_{spp\pm}$. Such kind of transient meta-grating coupling process can be described by replacing $|\vec{k}_0|sin\theta$ with $|\vec{k}_{spp}|sin\theta$ in an equation of $k_{spp} = |\vec{k}_0|sin\theta \pm |\vec{k}_g|$ [28]. As a result, the two diffracted surface plasmons can be achieved by $k_{\pm} = |\vec{k}_{spp}|sin \pm |\vec{k}_g|$, where $k_{\pm} = |\vec{k}_{spp\pm}|sin\gamma_{\pm}$ and γ is the diffraction angle ($\left|\vec{k}_{spp}\right| = |\vec{k}_{spp\pm}|$). Here $\theta = 0°$ is an incident angle of the propagating surface plasmon with respect to the transient meta-grating orientation. After series of the subsequent laser energy relaxations, three sets of periodic nanogrooves can be eventually obtained via the laser ablation processes, resulting in a spatial distribution of 2D nanotriangle structure arrays on the sample surface.

The formation of nanowires around the triangle structure unit for the case of 10^{-3} Pa, is attributed to the surface tension of the thermally induced thin liquid metal film in the nanogroove regions, whose shrinking effect can lead to the film fragmentation that then condenses into nanowires. Under the condition of 1 atm, heat transfer of the surrounding air is important and accelerates the solidification process of the molten surface. As a result, there is no enough time for the liquid film fragmentation before the re-solidification in the case of 1 atm. (Note: according to fragmentation criterion for the liquid phase, the time to fracture is increased for lower temperatures [29].). As a matter of fact, the heat transfer of the surrounding air can also be seen by the nanogroove depths measured under different ambient circumstances, i.e., the lower the air pressure, the more laser energy remains in the material, and the larger ablation depth can be made.

As for the measured dramatic decrease in the optical reflectivity of the tungsten surface with 2D nanotriangle structures, it can be attributed to the significant local-field enhancement on the edges and tips of the triangular structures [30]. Some previous studies also have shown that the local field enhancement of the nanotriangle structures is much stronger than that of the normal types of nanostructures [31,32]. For the 2D triangle structure arrays fabricated in high vacuum conditions, the resultant ablation groove depth and nanowire distribution is believed to further improve the capture of the incident photons [25], which consequently leads to a slight difference in the reflectivity between cases of 1 atm and 10^{-3} Pa.

Optics EXPRESS

4. Conclusions

In conclusion, we have introduced an unpreceding method to directly fabricate 2D arrays of periodic nanotriangle structures on the bulk hard material surfaces of tungsten, only by irradiation of collinear two femtosecond laser beams linearly polarized in orthogonal directions without any masks. With decreasing ambient air pressure, the unit cell in 2D triangular structures has been observed to present smaller side length but larger modulation depth, and the side-face nanogrooves have been seen to cover with some nanowires under the condition of 10^{-3} Pa. Moreover, the spatial distribution of the structures also tends to be more uniform at lower air pressures. The measured reflection spectra have demonstrated that the tungsten surface with 2D arrays of nanoscale triangle structures can unprecedentedly reduce the optical reflection within the wavelength range of 400 nm - 1100 nm. Physically, the formation of such structure units has been attributed to the spatially crossed distribution of three groups of periodic ablation nanogrooves that are triggered by the excitation of surface plasmons from two time-delayed femtosecond laser pulses on the metal target. This study suggests a new phenomenon of nonlinear lithography during femtosecond laser-metal interaction and some potentials for the future design of structures and devices, especially exhibiting direct, large-area nanofabrication via a single-processing step.

Funding

National Key R & D Program of China (2017YFB1104700); National Natural Science Foundation of China (NSFC) (11674178); Natural Science Foundation of Tianjin (17JCZDJC37900).